# Use of a handheld low-cost sensor to explore the effect of urban design features on local-scale spatial and temporal air quality variability

Georgia Miskell, Jennifer A Salmond and David E Williams

MacDiarmid Institute for Advanced Materials and Nanotechnology, School of Chemical Sciences, University of Auckland; and School of Environment, The University of Auckland, Private Bag 92019, Auckland 1142, New Zealand

## Abstract

Portable low-cost instruments have been validated and used to measure ambient nitrogen dioxide ($NO_2$) at multiple sites over a small urban area with 20 minute time resolution. We use these results combined with land use regression (LUR) and rank correlation methods to explore the effects of traffic, urban design features, and local meteorology and atmosphere chemistry on small-scale spatio-temporal variations. We measured $NO_2$ at 45 sites around the downtown area of Vancouver, BC, in spring 2016, and constructed four different models: i) a model based on averaging concentrations observed at each site over the whole measurement period, and separate temporal models for ii) morning, iii) midday, and iv) afternoon. Redesign of the temporal models using the average model predictors as constants gave three 'hybrid' models that used both spatial and temporal variables. These accounted for approximately 50% of the total variation with mean absolute error ±5 ppb. Ranking sites by concentration and by change in concentration across the day showed a shift of high $NO_2$ concentrations across the central city from morning to afternoon. Locations could be identified in which $NO_2$ concentration was determined by the geography of the site, and others as ones in which the concentration changed markedly from morning to afternoon indicating the importance of temporal controls. Rank correlation results complemented LUR in identifying significant urban design variables that impacted $NO_2$ concentration. High variability across a relatively small space was partially described by predictor variables related to traffic (bus stop density, speed limits, traffic counts, distance to traffic lights), atmospheric chemistry (ozone, dew point), and environment (land use, trees). A high-density network recording continuously would be needed fully to capture local variations.

**Keywords (4):** land use regression, urban network, nitrogen dioxide, spatio-temporal

## 1. Introduction

Changes in urban planning and design of urban form at local to urban scales have the potential to mitigate air pollution problems in cities. However, complex interactions between emission patterns, the built environment, and meteorology mean that urban air quality is highly heterogeneous in time and space which makes it difficult to develop informed decisions as to best practice. Recent developments to develop micro-scale variants of land use regression models (LURs) have shown potential to provide insight into the linkages between air quality and urban design at local scales (Rao et al. 2014; Tunno et al. 2017). However, attempts directly to apply the traditional LUR models developed for larger scales to micro-scale environments have shown poor transferability between and within cities (Mukerjee et al. 2012; Weissert et al. submitted) suggesting that different urban features are important in determining air quality patterns at different spatial scales.

One limitation that neither traditional LUR nor these micro-scale versions have been able to resolve for spatially dense areas, is their reliance on temporally averaged data. This means that links between urban factors and short-term temporal variations in local scale air quality, which may be important in determining links between human exposure and urban design, are not well represented. Recent studies have shown it is possible to derive LUR models using data with improved temporal resolution using regulatory monitoring networks (Molter et al. 2010) or handheld sensors (Deville Cavellin et al. 2016). However, this can come at the cost of reduced spatial resolution. This trade-off between temporal and spatial resolution limits the ability effectively to link different land uses or urban features to local-scale air quality.

Here we propose to use the recent improvements in sensor technology which enable dense networks of reliable low-cost instruments that can measure at high temporal resolution (Wang et al. 2016) to explore further developments into local-scale LURs. These sensors enable us to include shorter-term, temporally dynamic controls such as meteorology or local traffic behavior as predictor variables, enabling the identification and modeling of pollutant hotspots which are associated with a particular event such as the morning rush hour (Michanowicz et al. 2016). The study develops multiple LUR models that cover different time periods (morning, midday, afternoon) and uses both static (set in space over time) and dynamic (change in space over time) predictor variables. We used portable sensors around the downtown area of Vancouver, BC, to measure nitrogen dioxide ($NO_2$). LURs were constructed for the static variables using site-averaged data and typical LUR methodology (ESCAPE, 2010; Henderson et al. 2007) and for the dynamic variables using specific data from each time period. Further, we investigated the importance of different variables and site locations throughout the day based on concentrations rankings (for both high and low values and for temporally

consistent and inconsistent), which can collectively help in understanding which urban elements best explain variability at different times over a small area. This has important implications for the evaluation of human exposure, air quality management initiatives and urban design decisions.

## 2. Methods and Materials

### 2.1 Background and context

Measurements were made around the downtown area of Vancouver, BC (49°15'N 123.6°6'W) during spring 2016 (in local areas Downtown, Fairview, Kitsilano, and West End). This area is 14.63 $km^2$ with population of 172,050 (Statistics Canada, 2011). Ambient $NO_2$ is a well-studied atmospheric pollutant, with high concentrations commonly measured within urban areas due to traffic emissions as the principal source (Kim Oanh et al. 2012). A seasonal cycle is present, with concentrations often higher during winter from reduced engine efficiency and less atmospheric mixing including increased observation of temperature inversions. There are also typically two daily peaks that correspond to commuting periods (Mayer, 1999). Two regulatory air quality stations are within the study area (Robson Square and Kitsilano), with only the Robson Square station operational during the measurement campaign. Vancouver has a good record of air pollution research, including a number of LUR studies (Henderson et al. 2007; Abernethy et al. 2013; Su et al. 2008; Wang et al. 2013). Typical predictor variables for $NO_2$ within these models have been traffic densities (both light and heavy vehicles), land uses, road lengths, building heights, and population densities, with Pearson correlation ($R^2$) values between 0.52 – 0.67.

### 2.2 Measurement campaign

Monitoring was carried out over 24 March – 21 April 2016, excluding weekends and public holidays. The time of the year was selected because historically concentrations over this period at Robson Square have been similar to annual averages. Instruments were handheld Aeroqual S500 to measure ambient $NO_2$ and ozone, ($O_3$ measured due to cross-interferences with $NO_2$ sensor), a BT-Q1000X GPS to measure latitude and longitude, and a Kestrel 4500 Pocket Weather Tracker to measure air temperature, relative humidity, wind speed, and dew point with instrument specifications in the S.I. We used one $NO_2$ and one $O_3$ instrument throughout the entire campaign. They were mounted together and measuring simultaneously. Both devices were set to record one-minute averaged measurements. They sampled the air

through similar Teflon inlets that were approximately 5 cm apart. The instruments were placed within a backpack with Teflon inlets to ensure consistency in measurement height. Ideally, sites would be monitored continuously in order to capture all spatio-temporal variation evenly, however logistical and resource constraints meant that this was not possible. The compromise was to sample locations during similar times across different days, and was similar to previous handheld LUR sensor work (Deville Cavellin et al. 2016). Each site was visited for 20 minutes at a time and visited during each of the three times: morning (between 08:00 and 11:00), midday (11:00-15:00) and afternoon (15:00-18:00). Sites were selected using results from previous Vancouver LUR work (Henderson et al. 2007), high-temporal LUR resolution work (Dons et al. 2014), and high-spatial resolution LUR work (Miskell et al. 2015). Areas with high variability in predictor variables were targeted and other sites added to achieve reasonably even spatial coverage. This resulted in 45 sites, with locations in spaces such as large parks, residential, high-rise commercial, or mixed-use shopping settings. Sites were divided into five areal sub-clusters to ensure that each site could be monitored within the required time frame (in S.I.). Traffic variables collected were counts of heavy (truck and buses) and light vehicles along the nearest road. All passing buses or trucks during sampling were counted, along with any passing car within an area where traffic loads were low (e.g. in quiet residential streets). We counted number of cars in busy areas by four one-minute periods throughout sampling. This was due both to the difficulty in counting over the entire sampling time with high traffic loads and that nearby traffic lights (phases around one-minute) caused regular patterns in passing traffic. These four counts were then added and multiplied by five to give a 20-minute estimate on number of passing cars. Notes were also made regarding the immediate surroundings and any events, such as presence of awnings or trees and any nearby construction work. Data from 19 weather underground (WU) stations (five with wind data) were linked to the five areal sub-clusters and medians derived for times when monitoring was completed to give an approximate state of the atmosphere at a wider spatial scale. Summaries on each WU cluster are provided in the S.I.

## 2.3 Sensor calibration

Field and laboratory calibration against the regulatory monitor and careful assessment of errors from sensors are critical to evaluate the reliability of the data. The device for $NO_2$ uses an electrochemical sensor, for which there is a significant interference by ozone (Deville Cavellin et al. 2016; Lin et al. 2015). A discussion on our handling of this interference is in the Supporting Information (S.I). Instruments were calibrated in the laboratory (Figure 1A)

showing the expected unit slope (see SI). It is important, however, to check this calibration validity in the field. To do this, we used the idea of a proxy measurement, introduced in (Miskell et al. 2016). We assumed that the distribution of $NO_2$ at the Robson Square reference station, located in the center of the study zone, over the entire monitoring length would have a similar mean and variance as that of the entire study data – i.e. the concatenated time series of all measurements from all measurement times at all measurement sites. Thus we calculated slope, $a_1$, and offset, $a_0$, to match the mean and variance of measured $NO_2$, after removing cross-interference from $O_3$ (see S.I.) to that at Robson Square, $C_{ref}$:.

$$C_{NO_2} = a_1\left(C_{ind} - C_{O_3}\right) + a_0 \tag{1}$$

$$a_1 = \sqrt{var\langle C_{ref}\rangle / var\langle C_{ind} - C_{O_3}\rangle} \qquad a_0 = \mu\langle C_{ref}\rangle - a_1\mu\langle C_{ind} - C_{O_3}\rangle \tag{2}$$

Where $C_{NO_2}$ denotes the concentration of $NO_2$ calculated from the measurements, $C_{ind}$ the concentration indicated by the hand-held $NO_2$ instrument, $C_{O_3}$the ozone concentration given by the hand-held ozone instrument, *var*< > denotes the variance, $\mu$< > the mean and $C_{ref}$ the concentration distribution for $NO_2$ obtained from the Robson Square reference instrument. Figure 1B shows the distribution of the raw field data, whilst figure 1C shows the Robson Square distribution and the matched field distribution, calculated from equations 1 and 2. . The expanded inset of Figure 1A compares the laboratory calibration to the field normalization. The field normalization in fact well describes the low concentration range laboratory data. However, considering the full data range, the instrument constant, *k* (see SI) may indeed have been changed by the field measurement setup. We confirmed that field alignment of the data was correct by measuring for a day at a site in a park, away from the city center and next to another reference station.

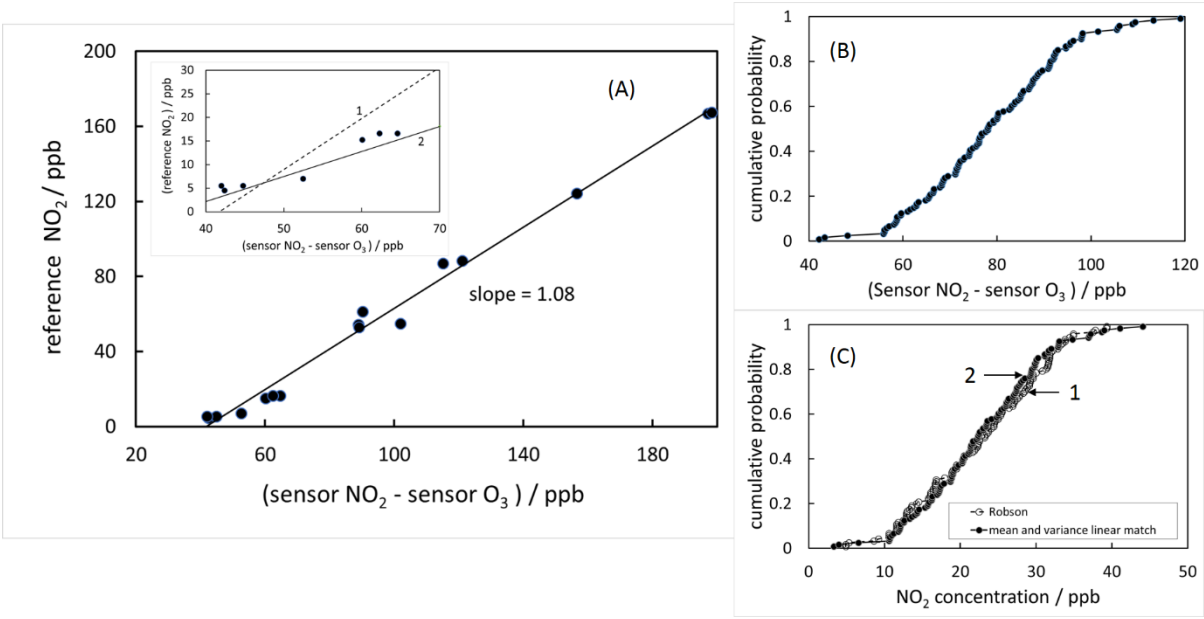


*Figure 1: A: laboratory and field calibration of the handheld $NO_2$ instrument. Inset: comparison of laboratory and field calibration at low concentrations. Points: low concentration range laboratory measurements from main diagram; Line 1: least-squares fit of entire concentration range, shown in main figure; Line 2: slope and intercept determined by matching mean and variance of the entire instrument measurement set to that measured at the Robson Square reference station. B: raw sensor data distribution for the entire measurement campaign; C: Field calibration alignment. 1: distribution of data at Robson Square for the period of the entire measurement campaign, for the times of measurement; 2: sensor data with slope and offset computed to match the Robson Square mean and variance.*

There was a fluctuation in the reading of the electrochemical sensor during field co-location which was traced to measurement noise on the signal. It varied over time with standard deviation of ±6 ppb at one-minute measurements, and ±1.5 ppb for 20-minute means. The estimated standard deviation in 20-minute median $NO_2$ concentrations using the sensor data in the present study, relative to a local reference station measurement, was ±3.3 ppb (s.d. of the difference between analyzer and corrected sensor measurements).

## 2.4 Data manipulation

Monitoring periods that had measurement standard deviations significantly greater than the estimated instrument error (>± 2 error) were removed from analysis as these locations were believed to be too impacted by local-scale activities. The occurrence of such activities – usually connected with internal combustion engines such as nearby seaplanes or lawn mowing – was verified from the observation log. This resulted in the removal of 13 observations, leaving $n$ = 122 non-averaged measurements and $n$ = 44 time-averaged locations. Since we carried out the study by visiting fixed sites at different times, the need for scaling of data to account for large-scale temporal variations over time was considered. For traditional LUR models, scaling of

measured concentrations is normally performed in order to remove the effect of global variation associated with the date and time of measurement that is unrelated to local variation. Since measurements were not taken simultaneously, such regional variations should be accounted and corrected for before inter-site comparisons on spatial variables can be made. The scaling approach used here was similar to that used in previous LUR work (Abernethy et al. 2013; Wang et al. 2013). Two correction factors were derived using the Robson Square station data, for time of day (estimate on hourly), and day of monitoring from the measured period (estimate on daily). Data outside of the measurement period (night-time and weekend) were removed in order to make valid correction factors for the monitored time (see S.I. for time correction breakdown). However, the question arises as to the appropriate reference site to use for scaling. This may not be important for measurements averaged over annual time periods, however for short time-scales studied here, the choice of scaling site is important as values derived from Robson Square (an urban station) were different to those derived from a large spatial scale estimate using pooled analyzer data from around the wider Vancouver area. This underlined the complexity in time-scaling results at the local-scale and the importance of a nearby continuous data source that can give a reasonable representation on both approximate hourly and daily patterns. Checks were made between the measured and temporally adjusted data to see if any bias was introduced by using selected adjustment factors given this potential subjectivity. The median difference between scaled and un-scaled was small (0.01 ppb) and 88% of differences were within 5 ppb. Therefore the data scaled to Robson Square using these two correction factors was used for the development of the ‘static’ model (spatial variable only) in order to provide better comparability across sites. As a check, a second ‘static’ LUR model was constructed using un-scaled data. The same explanatory variables were found, but with slightly poorer statistical performance. This suggested that the choice of scaling was not significantly influencing results.

## 2.5 Land use regression model development

Predictor variables were divided into two classes; static (those that did not change over time), and dynamic (those that did change) (Table 1). The static variables were used to construct a traditional LUR, where variables were collected using observations made during monitoring, web-based mapping services, or available GIS layers. This model followed previous LUR work where the temporal variability was smoothed out by using a single averaged measurement from all data for a given site. In total, there were 29 variables tested, with small buffer sizes offered to those relevant variables due to the high spatial density focus

of the study. Each site was placed into one of four broad land use categories to describe the surrounding urban environment (‘high-rise’, ‘low-rise’, ‘residential’, and ‘park’). This allowed us to include or remove any particular land use based on their significance on $NO_2$ variability, thus controlling for potential overfitting in the model caused by including non-significant land uses. Those land use types that were significant could then be simply identified and added to the model as a binary indicator. The dynamic variables were used to construct the dynamic LUR models, with variables collected using observations, or web data. In total, there were 11 dynamic variables tested. A number of predictor variables had sub-categories relating to different data sources (distinguished in Table 1 using subscripts). The static and dynamic models followed previously used methods for LUR development (ESCAPE, 2010). These methods are described briefly. All predictor variables were tested by univariate regression to the response ($NO_2$). The predictor variable with the highest $R^2$ and a correct *a priori* direction was selected first and included in the model. Next, all predictor variables were tested for collinearity to the selected predictor variable using correlation between those prediction variables. If this was found to be acceptable (here set to $< 0.6$ following previous work; ESCAPE, 2010) then this variable and the selected predictor were used to construct a multi regression model. The new model with the highest adjusted $R^2$ and with correct directions for both predictor variables was then selected. If the adjusted $R^2$ had increased by at least 0.01 to the previous model, then this new model was accepted, with these steps repeated across all available predictor variables until no further improvements could be found in the model fit. Model building used the R package ‘caret’ and followed standard techniques.

*Table 1: Selected static and dynamic predictor variable characteristics. * denotes those variables which were against the assumed direction.*

| **Variable** | **Symbol** | **Variable Description** | **Measurement Unit** | ***A priori* Direction of Effect** |
|---|---|---|---|---|
| *Static* | | | | |
| Land use: high-rise | LU:HR | Location surrounded by tall buildings by binary response | 1 = Y; 0 = N | + |
| Land use: low-rise | LU:LR | Location surrounded by low urban buildings (e.g. shops) by binary response | 1 = Y; 0 = N | + |
| Land-use: residential | LU:R | Location surrounded by houses by binary response | 1 = Y; 0 = N | - |
| Land-use: park | LU:P | Location surrounded by park or green space by binary response | 1 = Y; 0 = N | - |
| Intersection | Int. | Location nearby an intersection (within 20 m) | 1 = Y; 0 = N | + |
| Vegetation | V | Location nearby some vegetation such as tree (within 20 m) | 1 = Y; 0 = N | - |
| Cycle Lane | CL | Location beside a cycle lane | 1 = Y; 0 = N | - |
| Fountain | F | Location nearby an operating fountain | 1 = Y; 0 = N | - |
| Awning | A | Location underneath an awning | 1 = Y; 0 = N | + |
| Building height: high | BH:H | Observation of surrounding building heights (> 5 levels or approx. > 20 m) | 1 = Y; 0 = N | + |
| Building height: medium | BH:M | Observation of surrounding building heights (>3 levels, < 5 levels, or between approx. > 10, < 20 m) | 1 = Y; 0 = N | + |
| Building height: low | BH:L | Observation of surrounding building heights (< 3 levels, or < 10 m) | 1 = Y; 0 = N | - |
| Building height: none | BH:N | No buildings nearby | 1 = Y; 0 = N | - |
| Speed Limit | SL | Speed limit along nearest road | 1 = 50 km/h; 0 = 30 km/h | + |

| | | | | |
|---|---|---|---|---|
| Car Park | CP | Location nearby a large carpark space (within 50 m) | 1 = Y; 0 = N | + |
| Rd. Direction* | RD | Traffic direction along nearest road | 1 = Both ways; 0 = one-way | + |
| Rd. Orientation | RO | Direction of road | N, NE, E, SE, S, SW, W, NW | NA |
| Number of lanes | NL | Number of traffic lanes along nearest road | Count | + |
| Street Width | SW | Width of the nearest road | m | + |
| Dist. Rd | $Dist_R$ | Distance to nearest road | m | - |
| Dist. Traffic Lights[a] | Dist $TL_X$ | Distance to nearest traffic light | m | - |
| Dist. Water | $Dist_W$ | Distance to the harbor | m | + |
| Dist. Truck Route | $Dist_{TR}$ | Distance to nearest established truck route | m | - |
| Dist. Gardens* | $Dist_G$ | Distance to nearest community garden | m | + |
| Dist. Park | $Dist_P$ | Distance to nearest public park | m | + |
| Dist. Main Rd. | $Dist_{MR}$ | Location within 100 m of a major road | 1 = Y; 0 = N | + |
| Dist. Airport | $Dist_A$ | Distance to Vancouver International Airport | m | - |
| Dist. Rail Line | $Dist_{RL}$ | Distance to nearest active rail line | m | - |
| Rd. Length[b] | RL | Sum of road length within various buffer sizes[b] | m | + |
| Sum Bus Stops[b] | Sum $Bus_X$ | Sum of public bus stops within various buffer sizes[b] | Count | + |
| Bus Density[c] | BD | Number of public buses along nearest road per weekday | Count | + |
| *Dynamic* | | | | |
| Temperature[d] | $T_X$ | Air temperature | °C | - |

| | | | | |
|---|---|---|---|---|
| Dew Point[d] | $DP_X$ | Dew point | °C | - |
| Relative Humidity[d] | $RH_X$ | Relative humidity | % | + |
| Pressure[d] | $hPa_X$ | Air pressure | hPa | + |
| Wind Speed[d] | $WS_X$ | Wind speed | $ms^{-1}$ | - |
| Ozone[e] | $O_X$ | Ground-level ozone | ppb | $_{S, R}$: -; $_{T, T-1}$: + |
| Weather | W | Observation on weather | Clear, Cloudy, Overcast | NA |
| Sum Car | Car | Sum of cars along nearest road | Count | + |
| Sum Bus[f] | $Bus_X$ | Sum of buses along nearest road | Count | + |
| Sum Truck | Truck | Sum of trucks along nearest road | Count | + |
| Total Vehicles | Total | Sum of total vehicles (cars, buses, and trucks) along nearest road | Count | + |
| Truck Ratio | $Ratio_T$ | Ratio of sum of trucks to sum of total vehicles along nearest road | Count | + |
| Bus Ratio | $Ratio_B$ | Ratio of sum of buses to sum of total vehicles along nearest road | Count | + |
| Bus and Truck Ratio | $Ratio_{BT}$ | Ratio of both summed buses and trucks to sum of total vehicles along nearest road | Count | + |
| Hour | HR | Hour of day (0-24) | Hour | NA |
| Construction | C | Location nearby construction work | 1 = Y; 0 = N | + |

[a] Traffic lights were divided into fixed ($_F$), actuated ($_A$), and all.
[b] Buffers used were 50, 100, and 200 m.
[c] Bus density was calculated using public bus timetables.
[d] Meteorological data were divided into the different measurements ($_K$ or $_{WU}$).
[e] Ozone data were divided into the different measurements ($_S$: sensor, $_R$: Robson analyzer, $_T$: downwind analyzer, $_{T-1}$: downwind analyzer an hour earlier).
[f] Buses were divided into electric ($_E$), gas ($_G$), small ($_S$), and all.

The dynamic models used un-scaled data and initially followed a similar LUR development to the static model, with the inclusion of a day of the week (DoW) variable (Patton et al. 2014). We also explored a new idea, to exploit the results from the static model. The developed static model was added as a constant, or 'offset' to each of the dynamic models to give three hybrid models. These models then had similar independent variables, e.g. with different coefficients, to the dynamic model, along with a constant that was determined using coefficients from static variables at each site. This caused the hybrid models to have some latent, fixed variables within this constant that helped to add in both site-unique static and temporal impacts. For each monitoring period (morning, midday, afternoon), the static model prediction for that site was set as a fixed offset and then fitting of the dynamic variables proceeded. We label this redesigned dynamic model as a 'hybrid' model. Offsets, where a predictor variable has a known and set coefficient, can help boost model results as known controls can already be accounted for. The reason for this redesign was that longer-term models are often found to 'explain' more variation within the data because they use fixed urban elements and remove local-event impacts through smoothing. By exploiting this feature we can derive a model which uses the best features of both static and dynamic models to capture temporal and spatial elements (Miskell et al. 2015). Fixing the coefficients for the static variables allows for the relationship between concentrations and static variables to be accounted for within dynamic models, contains fewer independent predictor variables (which adversely impact standard diagnostic tests), and provides a lower likelihood of observing model overfitting (Eq. 3).

$$
\begin{aligned}
&Y_i = \alpha + [\,\gamma\,] + \textstyle\sum_{i=1}^{n} \beta X_i + \epsilon \sim \textit{independent, visible dynamic model} \\
&\qquad\qquad \downarrow \\
&[\gamma = \alpha_C + \textstyle\sum_{i=1}^{n} \beta_C X_i] \qquad\qquad \sim \textit{dependent, latent static model}
\end{aligned}
\tag{3}
$$

Where: $Y_i$ = dynamic $NO_2$ estimate, $X_i$ = dynamic variable observation, $\alpha$ = dynamic model offset (model independent), $\beta$ = dynamic variable coefficient (model independent), $i$ = number of predictor model terms, $\gamma$ = static offset (latent, constant), $\alpha_C$ =constant static offset, $\beta_C$ = constant static variable coefficient, $\epsilon$ = dynamic error term.

Standard LUR model diagnostics were checked using adjusted $R^2$, $p$-value, root mean square error – RMSE, mean absolute error – MAE for fit and accuracy; Moran's $I$ for residual spatial autocorrelation ($p < 0.05$); Shapiro-Wilk for normality testing ($p < 0.05$); Cook's

Distance for influential points ($D > 1$); and predictor variable correlations for multicollinearity ($\rho < 0.6$). External model validation was also completed using subsets of the data (leave-one-out cross validation and bootstrapping to test predictor coefficient stability), with adjusted $R^2$ and selected variables noted, along with spatial autocorrelation checks for clustering of selected sites. Each selected variable was tested for homoscedasticity and normality of the residuals against the appropriate response, with acceptable results and so each variable can be viewed as suitable for parametric regression.

## 2.6 Site ranking analysis

Site ranking by concentration focuses attention on those sites that are consistently low or high in concentration in comparison with others, and on those sites that show large changes in rank according to the time of measurement. Random measurement errors affect these analyses differently to regression analyses. For each measurement period (morning, midday, afternoon) sites were ranked according to the median, unscaled concentration. For each site, we also recorded rank range – the difference between the highest and the lowest of these three ranks. The cumulative distributions of rank and rank range were divided into three zones: high, buffer and low. A buffer was used in order to make our two top and bottom samples have differences that were significant with respect to the estimated standard deviation in the measurements. Based on our top and bottom samples having sizes of n = 10, these buffer sizes were around 50% of the sample. Thus, regression models using only values from either the selected 'high' and 'low' samples may identify those urban design elements that are associated to high and low values (either concentration or range rank), respectively. Thus, we were able to identify those sites that were temporally consistent – that is, sites where the dominant effects were associated with specific time-stable characteristics of the location - and those where temporal variations were particularly important. We were also able to identify specific characteristics of the sites and times associated with high and low values of the concentration by using rank correlation with predictor variables for those sites outside the buffer zone (i.e. definitively high and definitively low). Mann-Whitney U-tests were performed on all predictor variables for the top ten and bottom ten ranked sites to identify any significant elements that differentiated the high and low groups ($p < 0.05$). Checks were further made across the three time periods using Kruskal-Wallis tests to investigate any elements in the top and bottom ranked sites that may be unique for certain times ($p < 0.05$). Qualitative checks were also completed for possible explanations into what caused a location to have high or low concentrations throughout that day, or what caused a site to be impacted by time. Finally,

selected predictor variables for each LUR were joined into three separate clusters: traffic-related, urban design-related, and atmospheric-related to ascertain which time period was explained the most by which urban control.

## 3. Results

### 3.1 Data summary

A weekday daytime median $NO_2$ concentration of 15.3 ppb was observed at the Robson Square reference station over the whole length of the campaign, with values ranging from 5.4 to 42.4 ppb (Figure 1C). Thus, within the error estimates, the handheld sensors were well able reliably to resolve site differences. Table 2 collects the summary statistics.

*Table 2: Summary on the results from different data sources on air quality and meteorology during monitoring. Time is the time-frame resolution and SD is the standard deviation. Subscript symbols represent the different data sources (S = station data, WU = Weatherunderground data, K = Kestrel data).*

| **Data** | **Unit** | **Time** | **Min** | **Median** | **Max** | **Mean** | **SD** |
|---|---|---|---|---|---|---|---|
| Robson Square $NO_2$ | ppb | Hour | 4.9 | 23.2 | 39.3 | 22.8 | 8 |
| Aeroqual $NO_2$[a] | ppb | 20-min | 3.9 | 23.5 | 41 | 23.6[c] | 7.6[c] |
| Aeroqual $NO_2$[b] | ppb | 20-min | 10.1 | 22 | 34.7 | 22.5 | 5.6 |
| $Temperature_S$ | °C | Hour | 5.8 | 14 | 25.7 | 14.6 | 4.8 |
| $Temperature_{WU}$ | °C | 20-min | 9.6 | 15 | 25.7 | 15.8 | 4 |
| $Temperature_K$ | °C | 20-min | 8.5 | 16.7 | 29.6 | 17.3 | 4.4 |
| Wind $speed_S$ | $ms^{-1}$ | Hour | 0.2 | 2 | 4.8 | 2 | 1 |
| Wind $speed_{WU}$ | $ms^{-1}$ | Hour | 0 | 1.2 | 3.2 | 1.1 | 1 |
| Wind $speed_K$ | $ms^{-1}$ | 20-min | 0 | 0.4 | 2.1 | 0.4 | 0.4 |
| Relative $humidity_{WU}$ | % | 20-min | 8.6 | 61.5 | 83.9 | 59.7 | 12.6 |
| Relative $humidity_K$ | % | 20-min | 25.7 | 53.2 | 86.8 | 53.6 | 13.5 |
| $Pressure_{WU}$ | hPa | 20-min | 998.4 | 1016.8 | 1032.2 | 1014.3 | 8.6 |
| Dew $point_{WU}$ | °C | 20-min | 3.3 | 7.8 | 13.1 | 7.9 | 2.4 |
| Dew $point_K$ | °C | 20-min | 2.8 | 7.1 | 12.2 | 7.2 | 2.1 |

[a] This is the data recorded for each site, where no temporal adjustment has been made ($n$ = 122).
[b] This is the site-averaged data, where temporal adjustment has been applied ($n$ = 44).
[c] These values are not equal to the reference station values because some data were missing hence mean and std.dev. were evaluated over a different number of values from that used for calibration

The different time periods were somewhat similar in their summary statistics across all sites, with median (range) values of 26.5 (12.6 – 38.1), 22.6 (10.7 – 41), and 21.4 (3.9 – 39) for morning, midday, and afternoon monitoring respectively (where no temporal corrections were applied). One-way ANOVA had weak evidence of a difference ($p$ = 0.04), with Tukey confidence intervals showing morning to have higher values than the afternoon (difference = 4.3 ppb, $p$ = 0.03). Examination of the data in detail brings out a different story. Figure 2 shows the median concentration for each site, for the three measurement periods combined (used to build the "static" model) and for the morning, midday and afternoon periods separately. Spatio-temporal variability can be clearly observed.

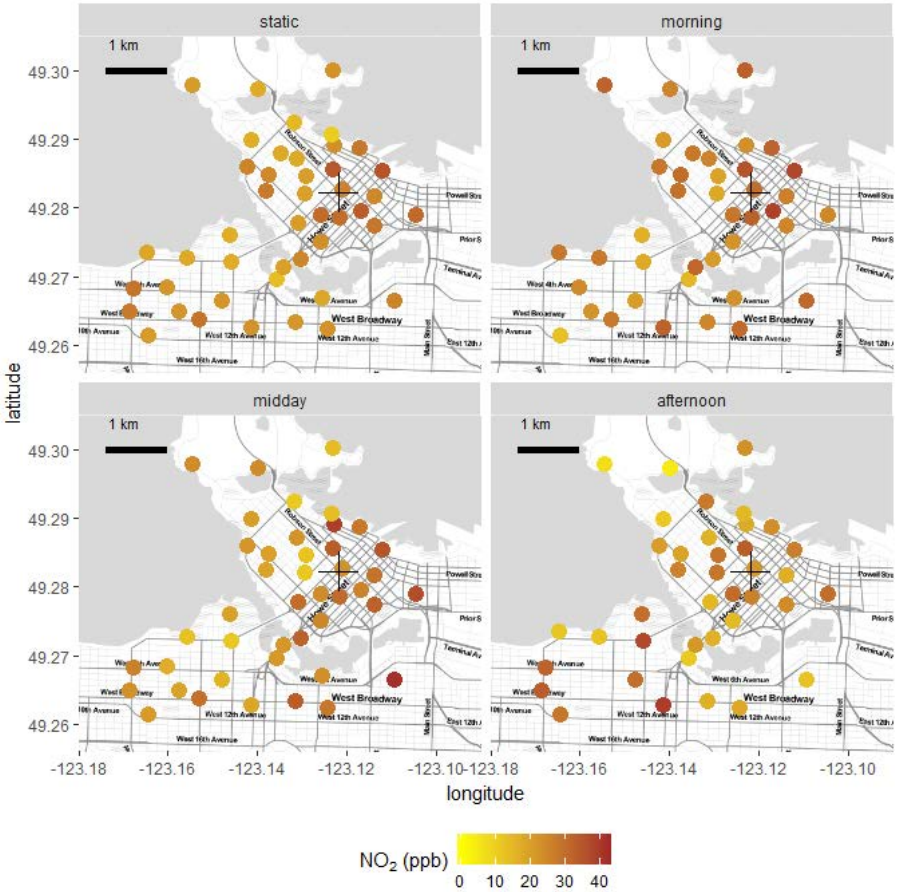


*Figure 2: Map of site median concentration (all time periods = 'static') and concentrations from measured time periods across the monitored area. The cross symbol denotes the Robson Square reference station.*

Figure 3 shows the top and bottom ranked sites for concentration for the different time periods. 'High' concentrations here were the top ten highest ranked concentrations for each time (AM values > 30.5 ppb; midday > 29.5 ppb; PM > 28 ppb). The converse also applied to 'low' concentrations (AM values < 22.15 ppb; midday < 18 ppb; PM < 15 ppb). These were selected so that some practical difference could be observed between the two groups, along

with providing reasonable sample sizes for later statistical tests, whilst ensuring that the buffer range of concentration was significantly larger than the estimated standard deviation in the measurement. Concentrations could be very different at different times of the day at sites that were spatially close. The site-averaged results tended to obscure these effects. The sites with the highest concentration tended to move south and east and those with the lowest concentration tended to move north and west as the day progressed. The effect could be simply due to the wind. Regional wind data showed wind speed increasing on average throughout the day, with the predominant direction coming from the north and west. Greater atmospheric mixing and movement would be expected toward the afternoon (S.I.).

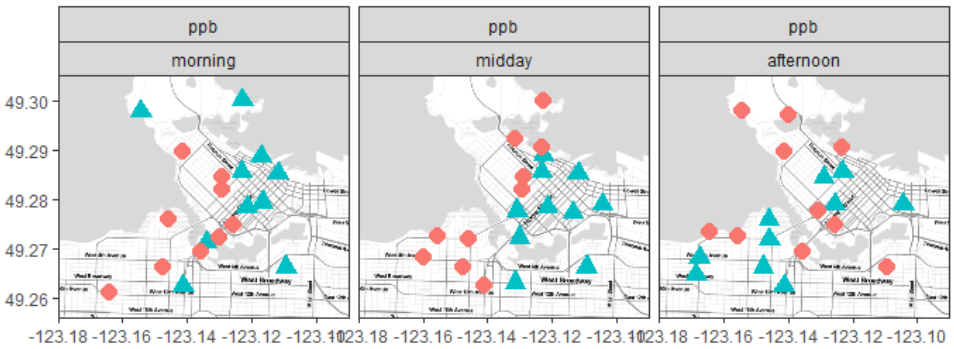


*Figure 3: top and bottom ten ranked sites for high and low concentrations for the different time periods using thresholds relative to each time (approx. high > 29 ppb and low approx. < 18 ppb). High concentration are blue triangles and low concentration are red circles.*

The rank range distribution identified those sites that were least and most variable across the day (Figure 4). The least variable ("site-important") tended to be localized in the high-rise urban center and on commuter routes in the center, and also in the more residential areas to the east. The most variable were around the edge of the main urban center, notably in the large park area to the north (Stanley Park) which is crossed by an extremely busy commuter route, and also around the bridges and commuter routes in the south of the study area. Variability in commuter traffic – more intense in the morning; more spread out in the afternoon and extending in time beyond the end of measurement for the day – might explain these results. Surprising observations are the large concentrations in Stanley Park that are well away from major roads. These observations were during the morning and were nearby water, and so may possibly be explained by passing container ships or nearby port activities coupled with a stable atmosphere.

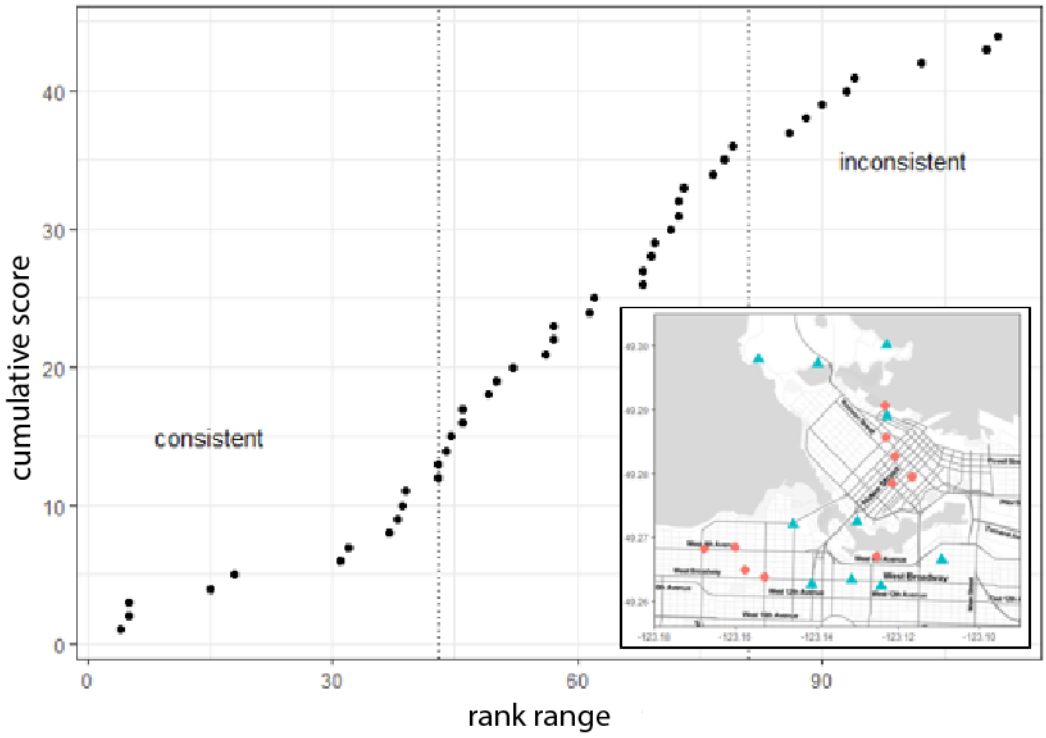


Figure 4: cumulative distribution of the rank range, identifying the top ten consistent (small rank range: site important) and inconsistent (large rank range: time important) locations. Inset: map of selected locations (blue triangles: time important; red circles: site important).

## 3.2 LUR results

The static LUR model identified three predictor variables (high-rise urban land use, sum of public bus stops within 200 m buffer, and speed limit) to collectively explain 53% of the observed variability in the temporally adjusted $NO_2$ data (Table 3; Figure 5A).

*Table 3: Results of the different LUR models. Symbols are in Table 1. n is the number of predictor variables in the model.*

| **Data** | **Model** | ***n*** | **$R^2$** | **Adj. $R^2$** | **Formula** |
|---|---|---|---|---|---|
| Static (*n* = 44) | Static | 3 | 0.56 | 0.53 | $NO_2$ = 16.7 + 3.9[LU:HR] + 0.8[Sum $Bus_{200}$] + 0.1[SL] |
| Morning (*n* = 40) | Dynamic | 3 | 0.45 | 0.41 | $NO_2$ = 24.4 + 0.2[$RH_K$] + (-0.8)[$DP_K$] +(-0.5)[$O_S$] |
| | Hybrid | - | 0.58 | 0.53 | $NO_2$ = 7.7 + offset[static model] + (-0.03)[$RH_K$] + (-0.3)[$DP_K$] + (-0.4)[$O_S$] |
| Midday (*n* = 43) | Dynamic | 2 | 0.37 | 0.34 | $NO_2$ = 26.3 + (-0.4)[$O_S$] + 0.5[bus] |
| | Hybrid | - | 0.48 | 0.46 | $NO_2$ = 3 + offset[static model] + (-0.3)[$O_S$] + 0.01[bus] |
| Afternoon (*n* = 39) | Dynamic | 3 | 0.5 | 0.47 | $NO_2$ = 25.1 + 0.01[car] + (-0.5)[$O_S$] + 3.5[HR] |
| | Hybrid | - | 0.61 | 0.58 | $NO_2$ = (-67.8) + offset[static model] + (-0.002)[car] + (-0.4)[$O_S$] + 4.5[HR] |

Univariate analysis on each of the four selected predictor variables had $R^2$ values over 0.2. Bus stop proximity is reasonable to associate with elevated $NO_2$ concentrations (Dons et al. 2014) because buses typically have diesel engines, which have higher $NO_2$ emissions than gasoline engines, and because stopping and restarting further increases $NO_2$ emissions (Chen et al. 2012). Our 'static' model results had some similarities to those results obtained in other LUR studies in Vancouver, where data were averaged over much longer times, with similar (where appropriate) predictor variables and model performance (Henderson et al. 2007; Su et al. 2008). This therefore further validates the use of low-cost, handheld instruments for this type of study. Measured data were then divided into each time period. The static model was applied to these measurements ($n$ = 122), and gave adjusted $R^2$ of 0.19 (Figure 5B). This model was unable to explain the higher and lower values that are often associated with time-specific activities. The result shows why a full spatio-temporal model is needed. The dynamic models, which had traffic as well as atmosphere variables (Table 3) but did not incorporate land use, performed better but not as well as the static model on the averaged data. Predictor coefficients were also standardized to assess their relative impact on $NO_2$ concentrations (each predictor coefficients fitted to $NO_2$ concentration normalized to give mean = 0 and standard deviation = 1). Standardized regression coefficients showed buses to have the highest relative impact on the static model (standardized coefficient = 0.43 compared to high-rise urban = 0.3 and speed limit = 0.2). Each dynamic model had the highest influence from co-located ozone, which was around double that of the other predictor variables (~ -0.55 compared to around 0.28). The hybrid models, where the static predictor variables were latent constants for each sites as described in Eq. 3, improved results for each dynamic model. Adjusted $R^2$ values improved to 0.46 - 0.58 (Figure 5C), with increases of at least $\Delta$0.11 for each model. Two variables in the hybrid models became insignificant and experienced changes in coefficient directions, however the largest impact on the final estimate was less than 1.5 ppb and so this was viewed as minor model overfitting. Coefficient direction changes, along with predictors becoming statistically insignificant, may be due to too many predictor variables being present in the hybrid model.

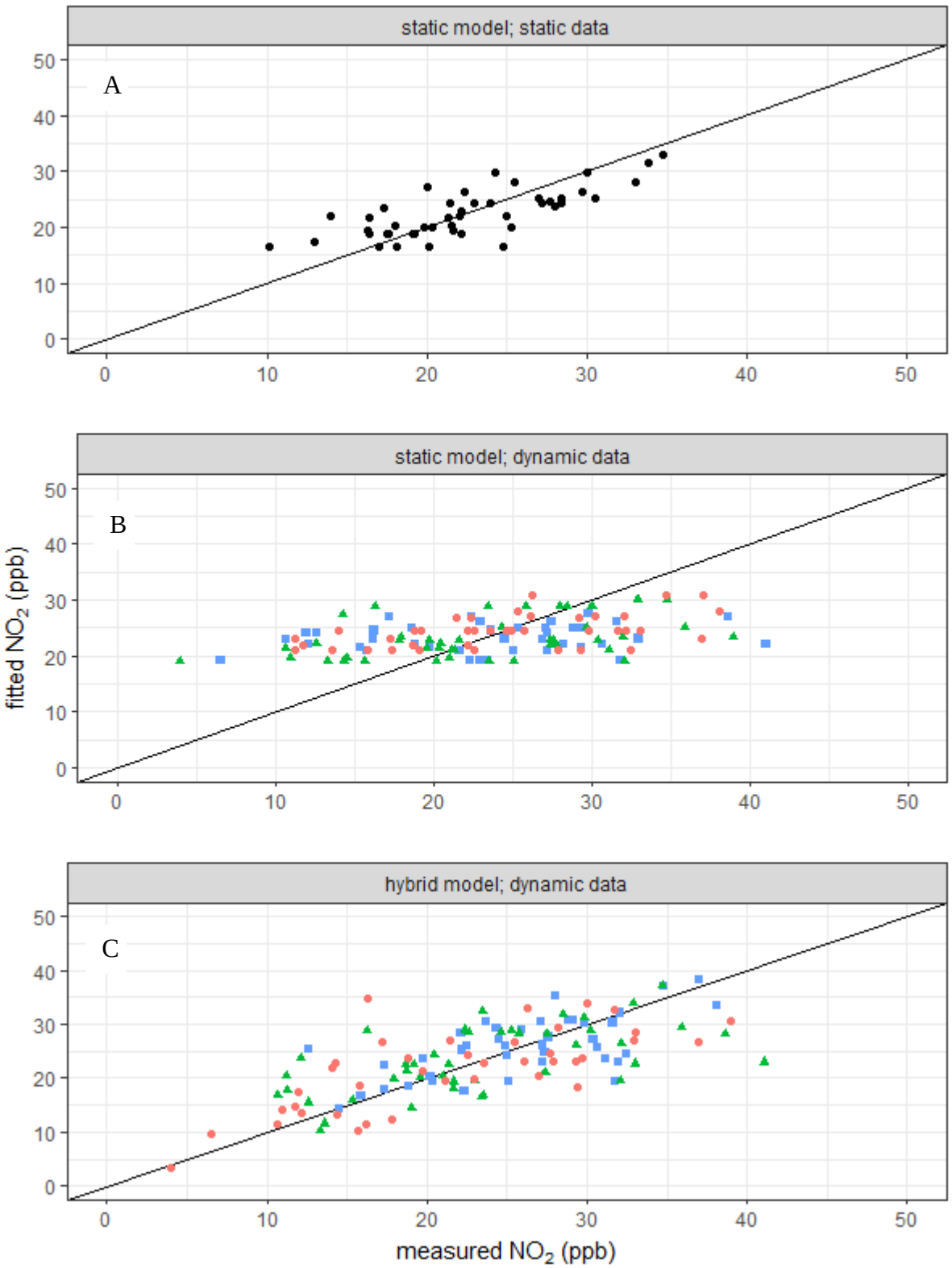


*Figure 5: fitted vs. observed concentrations for the different data-sets and LUR models. Black line is 1:1 line, pink circles are afternoon data, green triangles are midday data, and blue squares are morning data.*

The hybrid models predicted short-term concentrations reasonably well, and accounted for much of the observed temporal variations. A DoW factor was offered to the hybrid models

to check if this would improve results. The afternoon model had an increase in adjusted $R^2$, with concentration increases observed on Monday (*p*-value = 0.06). The improvement may be due to five new independent variables introduced, and so DoW were not added to the final model. Overall internal and external validation tests were found to be acceptable, and so each model was possible to use in explaining $NO_2$ variation around the downtown Vancouver area (Table 4). Prediction errors were reasonable with mean absolute differences typically up to 5 ppb between fitted and observed values. At some sites, however, the residuals were very large, implying perhaps the effect of short-term emission sources unaccounted for in the models. External predictor direction validation, where subsets of data were selected and the model fitted ten times to see if direction changed, were acceptable, with similar values to those found when using the full dataset. External validation typically had increased performance for the hybrid models than the dynamic models. The only obvious defect in the modelling was that clustering was found for the midday dynamic (Moran's $I$ $p < 0.001$) and hybrid ($p = 0.03$) residuals, with some over-estimation of concentrations toward the west of the monitored area (S.I.). The part of the unexplained variability due to the sensor measurement error was estimated as approximately 5-10% for each time period. Thus, overall, approximately 60% of the total variation was able to be explained.

*Table 4: Internal and external validation of the different LUR models. External validation is the average (S.D.) from 10 model runs using 20 randomly selected observations.*

| **Model** | **Internal Validation** | | | | | | **External Validation** | | | |
|---|---|---|---|---|---|---|---|---|---|---|
| **Test** | **RMSE (ppb)** | **MAE (ppb)** | **Moran's *I* *p*-value** | **LOOCV adj. $R^2$** | **Shapiro-Wilk *p*-value** | **Max. Cook's D** | **Adj. $R^2$** | **Predictor direction (%)** | **Model *p*-value** | **MAE** |
| Static | 3.7 | 2.9 | 0.67 | 0.55 | 0.57 | 0.14 | 0.54 (0.16) | 93 (14) | 0.009 (0.02) | 3.1 (0.3) |
| Morning dynamic | 4.5 | 3.5 | 0.87 | 0.41 | 0.45 | 0.25 | 0.34 (0.12) | 100 (0) | 0.04 (0.05) | 3.5 (0.5) |
| Morning hybrid | 4.8 | 3.6 | 0.19 | 0.47 | 0.73 | 0.23 | 0.53 (0.13) | 80 (17) | 0.005 (0.006) | 3.5 (0.7) |
| Midday dynamic | 6.1 | 4.6 | ~0 | 0.33 | 0.17 | 0.17 | 0.29 (0.13) | 100 (0) | 0.05 (0.06) | 4.4 (0.6) |
| Midday hybrid | 6.3 | 5 | 0.03 | 0.38 | 0.54 | 0.16 | 0.43 (0.09) | 75 (25) | 0.006 (0.008) | 5 (0.2) |
| Afternoon dynamic | 5.5 | 4.6 | 0.89 | 0.54 | 0.47 | 0.29 | 0.49 (0.12) | 97 (10) | 0.009 (0.02) | 4.2 (0.5) |
| Afternoon hybrid | 5.9 | 4.7 | 0.21 | 0.54 | 0.34 | 0.2 | 0.57 (0.17) | 77 (22) | 0.006 (0.01) | 4.3 (0.9) |

### 3.3 Site ranking analysis

We used site ranking to minimize the effect of instrument noise. For each measurement period, we took the sites that were identified as 'high' and 'low', then used rank correlation and the U-test to identify the significant variables. The spoke diagram, Figure 6, shows the results. This plot shows the rank correlation using the U-test results for the high and low concentration sites at each time period. The selected predictor variables (each 'spoke') were significant for at least one of the time periods when using only those selected high and low concentration sites. Correlations which are positive show those predictor variables that are higher for the high concentrations sites (e.g. the correlation for high-rise land use is around 0.5, and so gives evidence that sites within high-rise land uses show an increase in $NO_2$). In this diagram, the movement of the highest concentrations towards the south and east through the day is reflected in the change in sign of correlation of the variable 'longitude'. Associated with this is the variable 'Distance to Water' – those distances were generally less for sites in the south-west, and to a lesser extent the variable 'Land-Use: Residential' – residential areas dominate in the south-west of the study zone. This effect overwhelmed any other consequence of residential land use for this particular study zone and time. The strongest negative correlation is with ozone measured by the sensor itself. This is consistent with ozone consumption by vehicle-emitted NO producing $NO_2$. The ozone source for the downtown area of Vancouver would be marine air (Weissert et al. 2017). The other correlations with ozone downwind, ozone at the urban center (Robson Square) and $NO_2$ at Robson Square reflect the processes of ozone titration, photolytic ozone production and transport of $NO_2$ , NO and $O_3$. As well as the importance of high-rise buildings (variable LU:HR) the rank correlation identifies vegetation as a significant factor causing decrease of $NO_2$ and the presence of awnings as a factor tending to increase local $NO_2$. Distance from road correlates generally as expected. High atmospheric pressure tends to be correlated with anticyclonic conditions which leads to still air over the city and consequently lack of dispersion of pollutants. In an urban area, $NO_2$ is normally derived from oxidation of vehicle-emitted NO with ozone and hydroxyl radicals. Therefore traffic behaviors, downwind $O_3$, sunlight, temperature and water vapor pressure can be expected to determine concentrations (Tunno et al. 2016; Wang et al. 2016; Michanowicz et al. 2016; Dons et al. 2014). This work has shown general conformity to these expectations. In particular, it has highlighted the importance of local $O_3$ concentrations and how significant predictor variables can change over time to account for changing atmospheric conditions.

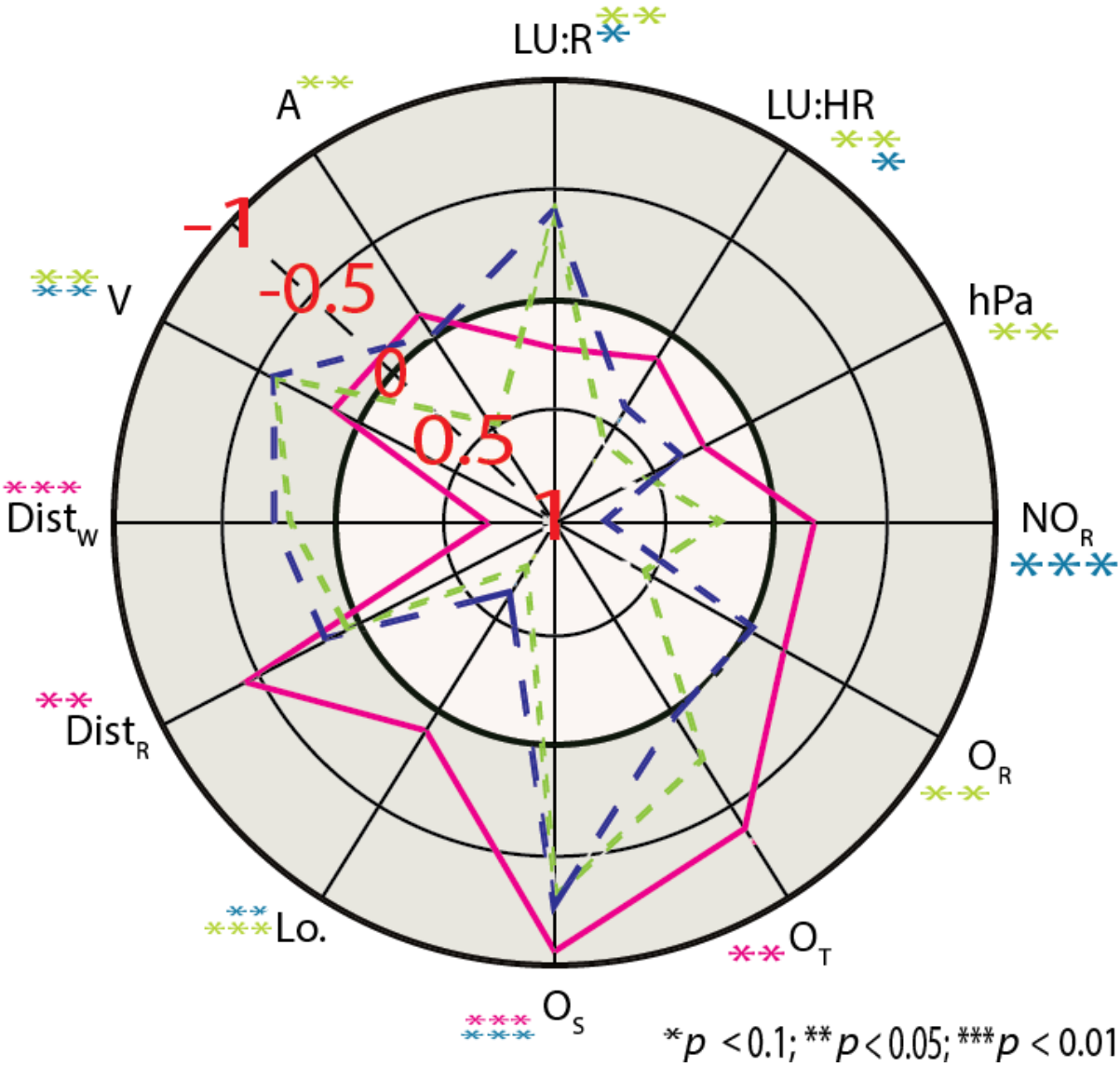


*Figure 6: radial plot of rank correlations for the top and bottom ranked concentrations over time (blue long dash = morning, green short dash = midday, and pink solid = afternoon). Predictor variable names are those in Table 1, along with Lo. = longitude, and $NO_R$ = Robson $NO_2$). Those sections in grey show negative correlations to $NO_2$ and those in white show positive correlations.*

The different predictor variables were grouped together by traffic, atmosphere (ozone concentration) and urban design controls, and used to see how much they explained the observed variability overall. The static model found 58% of the explained variation to be from traffic-related processes, especially buses. The morning data found urban design, traffic and atmospheric processes to describe 32%, 36% and 75% of the explained variability (overestimation due to collinearity between the groups), the midday data found urban design (46%) and atmosphere (63%) to be important, and afternoon found traffic (26%) and atmosphere (72%) to be important. From this, urban design variables were important controls on the morning and midday data, which had reduced by the afternoon. Traffic was important

during the morning and afternoon commuting periods, with the static model finding bus proxies to be the most significant determinant of elevated $NO_2$. The urban design elements that were most significantly associated with higher $NO_2$ concentrations were high-rise land uses, fewer nearby trees, and proximity to bus proxies (e.g. bus stops or lanes). Many of the low concentration sites were near cycle lanes, which may be a proxy for reduced traffic due to removal of traffic lanes or to the site being located off a main road where cycle lanes are often present. Locations that had consistently high concentrations throughout the day were around the built up downtown area. Unsurprisingly, major roads within the built-up area were consistently high. Comparison of sites with a consistent ranking across the day with those that were inconsistent in their ranking showed consistent sites to have higher exposure to buses (by bus lanes and bus stops) and nearby to main roads. These constitute steady emission sources. The sites where concentration varied significantly between the different measurement periods appeared to have greater traffic fluctuations, such as higher combined car, bus, and truck counts when concentrations were higher, which again appears sensible as these variables would be expected as the predominant emission source in an urban environment. Assessment of field notes also helped to shed light on some reasons for large variations in site ranking. For example, one location, 'False Creek', was nearby a concrete factory, which was working when this site was visited during the midday period. This measurement was significantly higher than that recorded on the other two visits. Those measurements that were labeled as 'unstable' ($n$ = 10) due to high variability on the one-minute timescale were further examined for specific events using field notes. Some locations were found to have nearby combustion sources that may have accounted for this extreme short-term variability (e.g. lawn mowing, smokers, sea planes, and construction).

We only measured during daytime weekday periods, and so spatio-temporal patterns can be expected to change outside of these times. A continuous network may assist in model improvements (both static and dynamic), firstly by fitting a suitable offset from an appropriate 'urban background' site for different times of the day, secondly by allowing for further variable exploration which might be accountable for this unknown yet identified variability, and thirdly by ascertaining if specific differences in timing of measurements influenced results. Continuous monitoring would also be useful for identifying other potential variables that straddle the dynamic/static definitions such as DoW and times of day. To operate a continuous network that delivers dynamic models would require other autonomous datasets such as traffic counters and meteorological stations at some sites or in proximity.

## 4. Conclusions

This work has illustrated that air quality variations across a small space may have different controls and patterns than those found at larger-scales. We have shown that, with appropriate field calibration, LUR models constructed as hybrids of static and dynamic variables can be built using portable low-cost sensors as the measurement tool. With a sufficient number of measurement locations, rank correlation methods also proved powerful in identifying control variables. This is a relatively simple technique to use to understand much about the different factors influencing concentrations and to explore mitigation through urban design. Results for the different models found a mix of traffic, urban design and meteorological variables affecting concentrations, with adjusted $R^2$ values of 0.53 for the static model and 0.46 - 0.58 for the hybrid models. It is however clear that these models do not adequately capture all observed variability as approximately 40% remained unexplained. For reliable assessment of exposure, continuous monitoring with an adequately dense network of low-cost devices would seem to be required.

## 5. Acknowledgements

The authors would like to thank Callaghan Innovation (contract AIRQU1301/34810), MacDiarmid Institute, and the New Zealand Ministry of Business and Employment (contract UOAX1413) for funding, Metro Vancouver for providing analyzer data, Lita Lee (Aeroqual Ltd) for the laboratory calibration, and Sam Mills for fieldwork assistance

## 6. References

Abernethy, R. C., Allen, R. W., McKendry, I. G., & Brauer, M. (**2013**). A land use regression model for ultrafine particles in Vancouver, Canada. *Environmental Science and Technology, 47(10)*, 5217-5225.

British Columbia Ministry of Environment. *BC Air Data Archive*. Retrieved from https://envistaweb.env.gov.bc.ca/

Chen, A., Watson, J. G., Chow, J. C., Green, M. C., Inouye, D., & Dick, K. (**2012**). Wintertime particulate pollution episodes in an urban valley of the western US: A case study. *Atmospheric Chemistry and Physics, 12(21)*, 10051-10064.

Deville Cavellin, L., Weichenthal, S., Tack, R., Ragettli, M. S., Smargiassi, A., & Hatzopoulou, M. (**2016**). Investigating the use of portable air pollution sensors to capture the spatial variability of traffic-related air pollution. *Environmental Science and Technology, 50(1)*, 313-320.

Dons, E., Van Poppel, M., Int Panis, L., De Prins, S., Berghmans, P., Koppen, G., & Matheeussen, C. (**2014**). Land use regression models as a tool for short, medium and long term exposure to traffic related air pollution. *Science of the Total Environment, 476-477*, 378-386.

ESCAPE. (**2010**). *ESCAPE exposure assessment manual*. Retrieved from http://www.escapeproject.eu/manuals/ESCAPE_Exposure-manualv9.pdf

Henderson, S. B., Beckerman, B., Jerrett, M., & Brauer, M. (**2007**). Application of land use regression to estimate static concentrations of traffic-related nitrogen oxides and fine particulate matter. *Environmental Science and Technology, 41(7),* 2422-2428.

Kim Oanh, N. T., Kongpran, J., Hang, N. T., Parkpian, P., Hung, N. T. Q., Lee, S. -., & Bae, G. -. (**2013**). Characterization of gaseous pollutants and PM2.5 at fixed roadsides and along vehicle traveling routes in Bangkok metropolitan region. *Atmospheric Environment, 77,* 674-685.

Kuhn, M. (**2010**). *caret: Classification and Regression Training*. R package version 6.0-73 https://cran.r-project.org/package=caret

Lin, C., Gillespie, J., Schuder, M. D., Duberstein, W., Beverland, I. J., & Heal, M. R. (**2015**). Evaluation and calibration of aeroqual series 500 portable gas sensors for accurate measurement of ambient ozone and nitrogen dioxide. *Atmospheric Environment, 100,* 111-116.

Mayer, H. (**1999**). Air pollution in cities. *Atmospheric Environment, 33(24-25),* 4029-4037.

Michanowicz, D. R., Shmool, J. L. C., Cambal, L., Tunno, B. J., Gillooly, S., Olson Hunt, M. J., . . . Clougherty, J. E. (**2016**). A hybrid land use regression/line-source dispersion model for predicting intra-urban $NO_2$. *Transportation Research Part D: Transport and Environment, 43,* 181-191.

Miskell, G., Salmond, J., Longley, I., & Dirks, K. N. (**2015**). A novel approach in quantifying the effect of urban design features on local-scale air pollution in central urban areas. *Environmental Science and Technology, 49(15),* 9004-9011.

Mölter, A., Lindley, S., de Vocht, F., Simpson, A., & Agius, R. (**2010**). Modelling air pollution for epidemiologic research - part II: Predicting temporal variation through land use regression. *Science of the Total Environment, 409(1),* 211-217.

Mukerjee, S., Smith, L., Neas, L., & Norris, G. (**2012**). Evaluation of land use regression models for nitrogen dioxide and benzene in four us cities. *The Scientific World Journal*, 2012.

Patton, A. P., Collins, C., Naumova, E. N., Zamore, W., Brugge, D., & Durant, J. L. (**2014**). An hourly regression model for ultrafine particles in a near-highway urban area. *Environmental Science and Technology, 48(6),* 3272-3280.

Rao, M., George, L. A., Rosenstiel, T. N., Shandas, V., & Dinno, A. (**2014**). Assessing the relationship among urban trees, nitrogen dioxide, and respiratory health. *Environmental Pollution, 194,* 96-104.

Statistics Canada. (**2011**). *Census local area profiles.* Retrieved from http://data.vancouver.ca/datacatalogue/censusLocalAreaProfiles2011

Su, J. G., Brauer, M., & Buzzelli, M. (**2008**). Estimating urban morphometry at the neighborhood scale for improvement in modeling static average air pollution concentrations. *Atmospheric Environment, 42(34),* 7884-7893.

Tunno, B. J., Shmool, J. L. C., Michanowicz, D. R., Tripathy, S., Chubb, L. G., et al (**2016**). Spatial variation in diesel-related elemental and organic $PM_{2.5}$ components during workweek hours across a downtown core. *Science of the Total Environment, 573,* 27-38.

Wang, R., Henderson, S. B., Sbihi, H., Allen, R. W., & Brauer, M. (**2013**). Temporal stability of land use regression models for traffic-related air pollution. *Atmospheric Environment, 64,* 312-319.

Wang, A., Fallah-Shorshani, M., Xu, J., & Hatzopoulou, M. (**2016**). Characterizing near-road air pollution using local-scale emission and dispersion models and validation against in-situ measurements. *Atmospheric Environment, 142,* 452-464.

Weissert, L.F., Salmond, J.A., Miskell, G., Alavi-Shoshtari, M., Grange, S.K., et al. (**2017**). Use of a dense monitoring network of low-cost instruments to observe local changes in the diurnal ozone cycles as marine air passes over a geographically isolated urban center. *Science of the Total Environment, 575,* 67-78.

Weisset, L.F., Salmond, J.A., Miskell, G., Alavi-Shoshtari, M., & Williams, D.E. (**submitted**). Development of a microscale land use regression model for predicting $NO_2$ concentrations at a heavy trafficked suburban area in Auckland, NZ, to Science of the Total Environment.